

# Replicated arrays of hybrid elements for application in a low-cost micro-spectrometer array

S. TRAUT<sup>†</sup>, M. ROSSI<sup>‡</sup> and H. P. HERZIG<sup>†</sup>

<sup>†</sup> Institute of Microtechnology, University of Neuchâtel, Rue A. L. Breguet 2, 2000 Neuchâtel, Switzerland

<sup>‡</sup> Centre Suisse d'Electronique et de Microtechnique CSEM, Badenerstrasse 569, 8048 Zürich, Switzerland

**Abstract.** We report on the fabrication and characterization of replicated hybrid elements for low-cost micro-spectrometer array applications. An array of hybrid elements, where one surface combines the fairly large dimensions of refractive microlenses with the submicron features of a diffraction grating, was successfully replicated by hot embossing. The parameters are: lens diameter = 990  $\mu\text{m}$ , height = 60  $\mu\text{m}$ , grating period = 1  $\mu\text{m}$ , linewidth = 300 nm and grating depth = 2  $\mu\text{m}$ . These replicated spectrometer elements showed a maximum resolution of 2.25 nm and a stray-light suppression better than 30 dB.

## 1. Introduction

Today, R&D efforts in optical demultiplexing systems, such as used for chemical analysis or in telecommunications, are directed towards miniaturization and cost reduction. Micro-optics combined with replication technologies provide obvious solutions particularly for parallel processing with array systems [1]. Hybrid (refractive/diffractive) elements [2, 3] offer the possibility to combine two functions in one element, and are therefore suitable for the application in miniaturized spectrometer systems [4]. Refractive microlenses with a diffraction grating on the curved surface combine the focusing and the dispersion necessary for any demultiplexing system essentially on one transmitting surface. Replication of these elements allows mass production [5] and hence yields a low-cost system, such as the spectrometer array system for chemical analysis proposed earlier [6]. The aim of this work was to show that it is possible to fabricate and to replicate arrays of lenses with fairly large dimensions (lens diameter = 990  $\mu\text{m}$ , height = 60  $\mu\text{m}$ ) and very fine structures on top of the surface (grating period = 1  $\mu\text{m}$ ) with sufficient quality for its application in an spectrometer array system.

## 2. Fabrication and replication

The process steps for the fabrication of the elements are schematically shown in figure 1. Refractive microlens arrays are fabricated by the melting resist technique [7] in photoresist on a glass substrate. The single lens has a diameter 990  $\mu\text{m}$  and a height of 60  $\mu\text{m}$ . The calculated numerical aperture of the single lens is 0.12. The

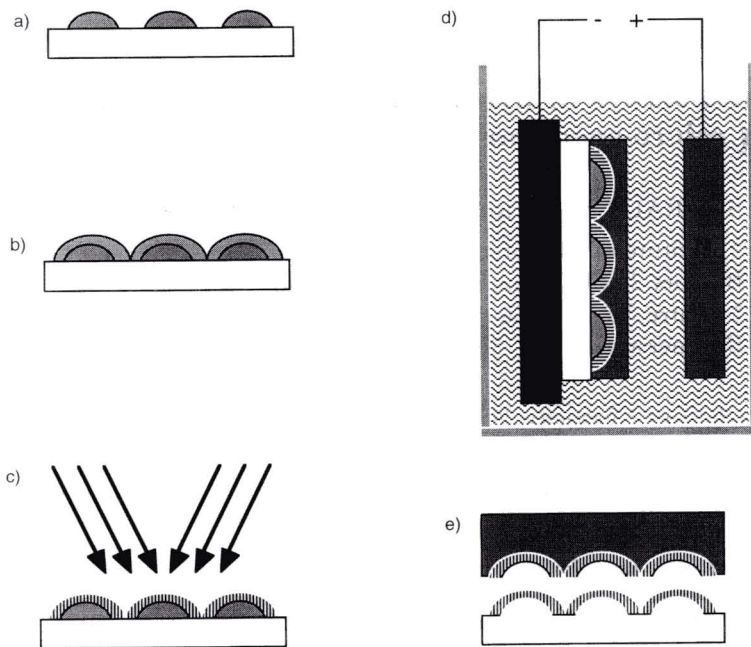


Figure 1. Fabrication process of the hybrid element (a) microlens array fabrication, (b) photoresist coating of the array, (c) recording of the grating, (d) electroforming of the element and (e) replication by hot embossing.

lens arrays are then spin-coated with photoresist (AZ1518, Suess RC8). A diffraction grating with a grating period of  $1\ \mu\text{m}$  is subsequently recorded by two-beam interference ( $\text{Kr}^{++}$ ,  $\lambda = 413\ \text{nm}$ ). Details of this fabrication process of the element in photoresist are presented in [6]. The element is then electroformed to a nickel shim and replicated onto polycarbonate (PCEurople) by hot embossing [8, 9].

Figure 2 (a) shows the SEM (scanning electron microscopy) image of a part of the replicated element. Figure 2 (b) shows the magnified replicated grating on top of a microlens. The photographs show the good quality of the replication for the lens as well as for the grating. The deep submicrometer features of the grating (linewidth =  $300\ \text{nm}$ , depth =  $2\ \mu\text{m}$ ) are replicated with high precision. The SEM picture shows the distinct boundaries between the lens surface and the grating.

The replicated grating exhibits only small defects in the centre of the microlenses and on a ring around the lens. Figure 3 shows an example of grating defects in the centre of a microlens. The Ni shim does not exhibit these defects. For its application as an element in a spectrometer system, however, these defects have only little influence on the performance. The defective parts of the grating, which are outside of the lens, are not utilized for the dispersion. The defective area in the centre of the microlens is very small compared to the entire lens surface. We therefore assume that its contribution to the stray light in the spectrometer system is negligible at this stage compared to other sources of stray light. The lens properties were measured with a Mach-Zehnder Interferometer from Mykos (Prof. Schwider) [10]. The measured quantity is the deviation of the wavefront

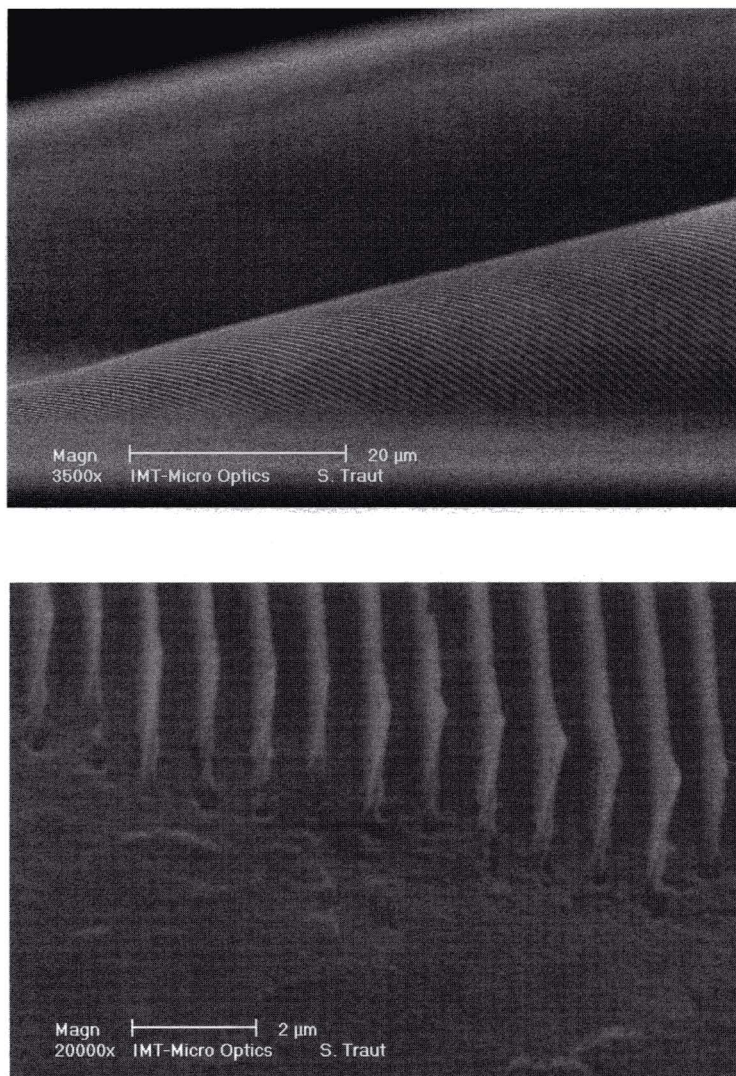


Figure 2. Scanning electron microscopy image: (a) part of a replicated hybrid element (990 μm lens diameter) and (b) grating on top of the refractive microlens (period = 1 μm, linewidth = 300 nm, depth = 2 μm).

generated by the microlens from an ideal spherical wavefront in  $\lambda$  (rms). The wavefront of the hybrid element in photoresist exhibited a deviation of  $1.13\lambda$ . For the replicated element we measured the deviation to be  $0.89\lambda$ . PCEurope has a lower refractive index than photoresist and therefore yields lower spherical aberration than photoresist for two lenses that are identical in shape. Furthermore, we assume that the melting process for the fabrication of the microlenses leads to a change in material properties of the photoresist, which is not homogeneous throughout the lens. A non-homogeneous index of refraction would also change the optical properties of the microlens. However, for a numerical estimation on the actual influence of this, further experiments would have to be performed.



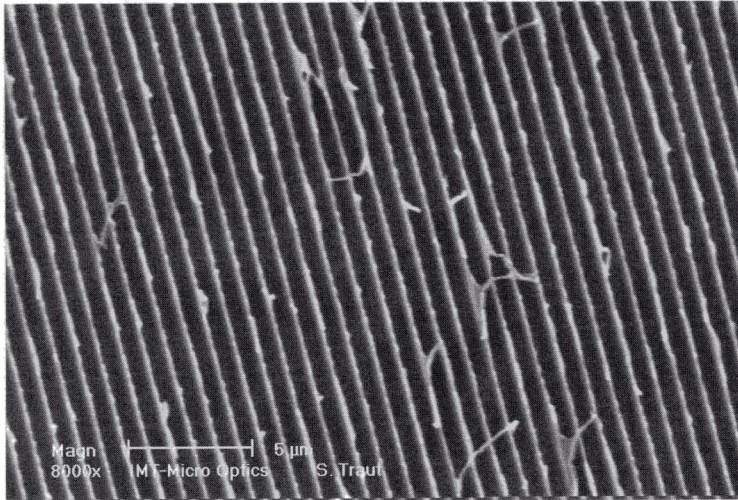


Figure 3. Example of grating defects in the centre of a microlens.

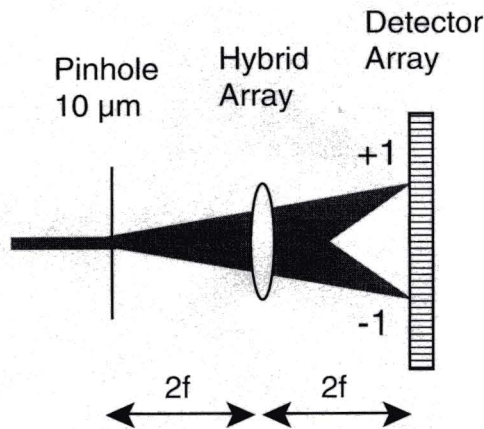
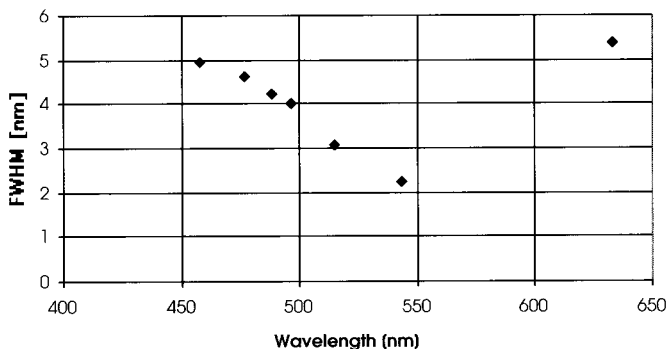


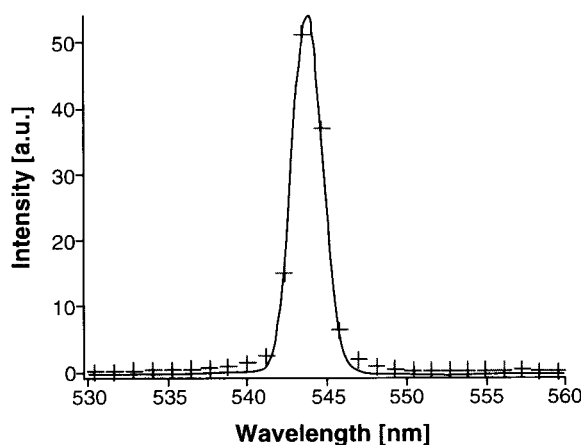
Figure 4. Spectrometer set-up with a pinhole for the characterization of the hybrid element.

### 3. Characterization for spectrometer applications

The characteristics of the replicated elements are measured with respect to its implementation in a spectrometer system. The two parameters measured were resolution and stray-light suppression. The spectrometer set-up for these measurements consisted of the hybrid element set-up in a 1:1 imaging system between a  $10\ \mu\text{m}$  pinhole and a one-dimensional detector array (Hamamatsu,  $25\ \mu\text{m}$  pitch,  $16\ \mu\text{m}$  width) as shown in figure 4. The detector is placed parallel with respect to the plane of the element and the pinhole is aligned on the optical axis of the microlens. Note that the detector pixels are of rectangular shape, which is ideal for a set-up using a slit, but increases the relative contribution of stray light for a round pinhole. An  $\text{Ar}^+$  laser and two HeNe lasers are used to generate different wavelengths for characterization. The lines of the  $\text{Ar}^+$  used were  $\lambda = 457.9\ \text{nm}$ ,  $476.5\ \text{nm}$ ,  $488\ \text{nm}$ ,  $496.5\ \text{nm}$  and  $514.5\ \text{nm}$  and the HeNe lines were  $543.5\ \text{nm}$  and



(a)



(b)

Figure 5. (a) Resolution measurements for the different wavelengths of an  $\text{Ar}^+$  and two HeNe lasers (543.5 nm and 632.8 nm); (b) fit of a Gaussian function to the intensity data of the resolution measurement for  $\lambda = 543.5$  nm.

632.8 nm. The spectrometer set-up is aligned (on the optical axis) for maximum resolution at the centre of the wavelength range of interest and the degradation of the resolution is observed towards both sides of the spectrum. The resulting intensity pattern for the single wavelengths are fitted to a Gaussian function and the resolution is given by the Rayleigh criterion (FWHM of the fitted Gauss). We chose the centre in the mid-visible region of the spectrum at  $\lambda = 543.5$  nm. The resolution at this wavelength is at a maximum of 2.25 nm (see figure 5 (a)). The resolution curve then degrades to both ends of the spectrum but remains below 6 nm for the entire measured bandwidth of 458–633 nm. Figure 5 (b) shows the Gaussian function which is fitted to the intensity data from the detector array for a wavelength of  $\lambda = 543.5$  nm. For the given system a further enhancement in resolution will soon be limited by the detector (pixel width, fill factor) rather than, e.g. the quality of the hybrid element.

For the stray-light suppression, two single lines ( $\lambda = 496.5$  nm and  $\lambda = 543.5$  nm) are again coupled into the spectrometer set-up and the intensity of the neighbouring

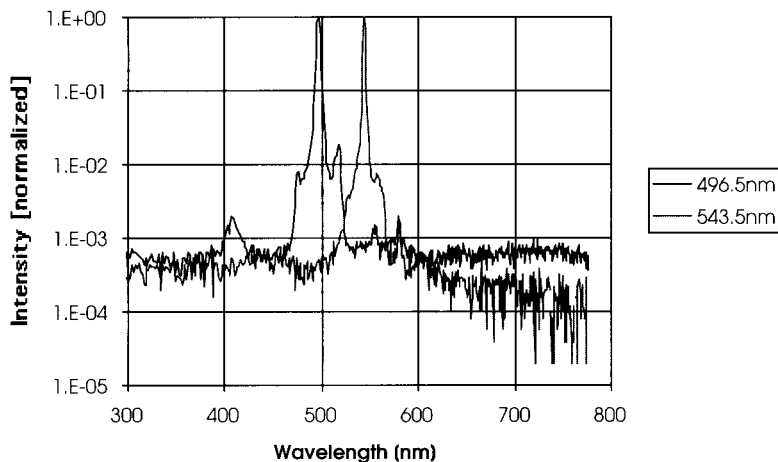


Figure 6. Stray-light suppression measurements with two single laser lines (496.5 nm and 543.5 nm).

pixels is analysed. The spectrum is plotted on a logarithmic scale with its peak value normalized to one. An attenuation of more than 30 dB is measured for both wavelengths (figure 6). Both parameters, stray-light as well as the resolution, have improved compared to the original sample in photoresist. We attribute this mainly to the enhancement in lens properties as stated earlier.

#### 4. Summary and conclusions

We successfully replicated an array of hybrid micro-optical elements in polycarbonate by hot embossing. The surface of the element combines the large features of the microlens array with submicron features of the diffraction grating. The lens, as well as the grating, which consists of lines as thin as 300 nm with a depth of 2  $\mu\text{m}$ , are well replicated with only minor defects in the centre of the single element. We see the application of this replicated hybrid element array predominantly in the field of low-cost miniaturized spectrometer arrays. The element provides a resolution of better than 6 nm for a bandwidth of at least 180 nm (measured bandwidth), with a maximum of 2.25 nm in the centre. The stray-light suppression is better than 30 dB. Limiting factors for even better performance are at this point the quality of the microlens arrays. Optimization of the fabrication process could lead to microlens arrays performing at the diffraction limit [11]. With that the resolution could yet be enhanced. A resolution of 1 nm should be feasible. However, as figure 5 (b) shows, the limiting factor will then be the detector array, which is required to have a smaller pitch between the pixels and a higher fill factor for a high resolution spectrometer system.

#### References

- [1] ROULET, J.-C., FLURI, K., VERPOORTE, E., VÖLKELE, R., HERZIG, H. P., DE ROOIJ, N. F., and DÄNDLIKER, R., 1998, *Micro Total Analysis Systems '98, Conference Proceedings* (Dordrecht: Kluwer Academic Publishers), pp. 287–290.

- [2] BEHRMANN, G. P., and MAIT, J. N., 1997, *Micro-Optics: Elements, Systems, and Applications*, edited by H. P. Herzig (London: Taylor & Francis), pp. 259–292.
- [3] SCHILLING, A., NUSSBAUM, PH., OSSMANN, CH., TRAUT, S., ROSSI, M., SCHIFT, H., and HERZIG, H. P., 1999, *Pure appl. Optics*, **1**, 244.
- [4] MÜLLER, C., and MOHR, J., 1993, *Interdisciplinary Sci. Rev.*, **18**, 273.
- [5] KLEY, E.-B., and SCHNABEL, B., 1995, *Proc. SPIE*, **2640**, 71.
- [6] TRAUT, S., and HERZIG, H. P., 2000, *Opt. eng.*, **39**, 290.
- [7] HUTLEY, M C., 1997, *Micro-Optics: Elements, Systems, and Applications*, edited by H. P. Herzig (London: Taylor & Francis), pp. 127–152.
- [8] GALE, M. T., 1997, *Diffraction Optics for Industrial and Commercial Applications*, edited by J. Turunen and F. Wyrowski (Berlin: Akademie Verlag), pp. 105–140.
- [9] GALE, M. T., 1997, *J. Image Sci. Technol.*, **41**, 211.
- [10] SICKINGER, H., and SCHWIDER, J., 1997, *Optik*, **107**, 26.
- [11] NUSSBAUM, PH., VÖLKEL, R., HERZIG, H. P., EISNER, M., and HASELBECK, S., 1997, *Pure appl. Optics*, **6**, 617.